concrete strength development (Lim 2019). The method could detect local structural damage by quantifying the variation in impedance responses measured before and after a damage event.

This study investigates the practicality of a smart rebar-aggregate for electromechanical impedance-based structural damage monitoring in prestressed concrete (PSC) anchorages.

2. IMPEDANCE-BASED CONCEPT FOR PSC-ANCHORAGE VIA EMBEDDED-PZT INTERFACE

The impedance-based technique has relied on the coupling of mechanical and electrical characteristics. The method employs a PZT patch to stimulate the monitored structure and to simultaneously obtain the structural vibrational responses under such excitation. The impedance can be calculated based on Liang (1994):

$$Z(\omega) = \left\{ i\omega A_p \left[\hat{\varepsilon}_{33}^{T} - \frac{1}{Z_a(\omega)/Z_s(\omega)+1} d_{31}^2 \hat{Y}_{11}^{E} \right] \right\}^{-1} \tag{1}$$

where i is the imaginary unit; ω denotes the excitation frequency; and A_p is the geometric parameters constant of the PZT patch; $\hat{\varepsilon}_{33}^{T}$, d_{31}, and $\hat{Y}_{11}^{E}$ are the complex dielectric constant at zero stress, the piezoelectric constant in 1-direction at zero stress, and the complex Young's modulus of PZT patch at zero electric fields. In Eq. (1), the electrical mechanical impedance, $Z(\omega)$, is a function of the impedance of the PZT patch, $Z_a(\omega)$ and that of the target structure, $Z_s(\omega)$. Thus, the change in structural characteristics (k, m, c) can be detected by the change in impedance signals.

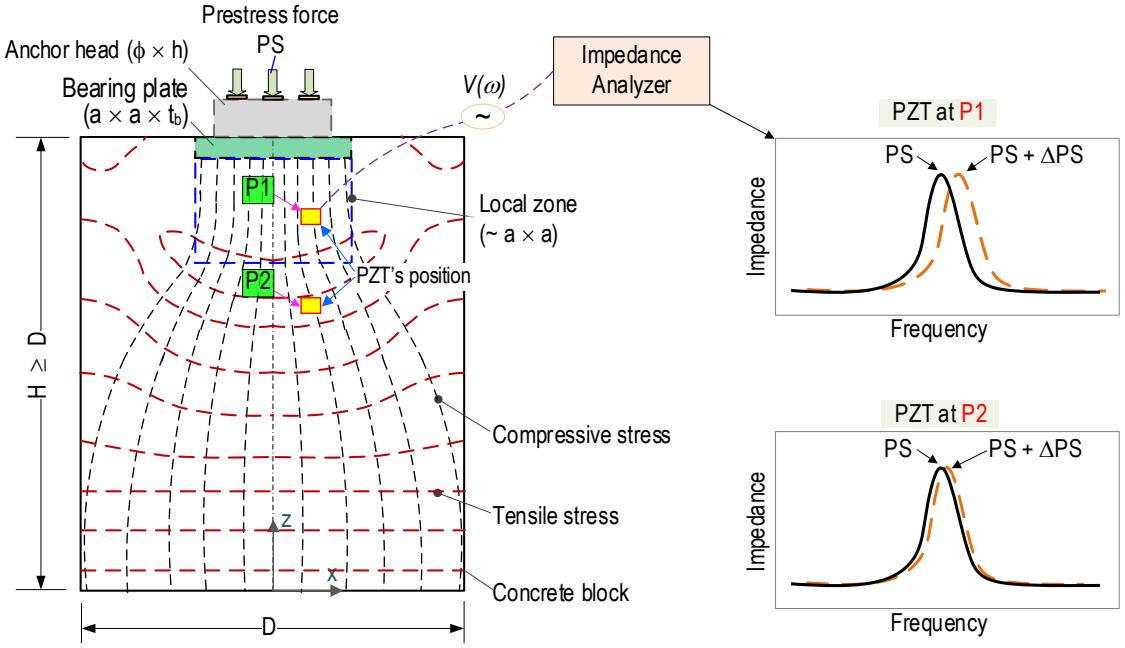

a) Anchorage zone with embedded-PZT sensors b) PZT impedance responses

Fig. 1 Impedance monitoring concept for anchorage zone via embedded-PZT sensor

As shown in Fig. 1a, the PSC anchorage consisted of an anchor head ($\phi \times h$), a bearing plate ($a \times a \times t_b$), and a concrete block ($D \times D \times H$) under prestress force PS. The stress distribution in the anchorage under PS can be examined in the local zone and the general zone, which can be found in Ro (2020). The local zone (~$a \times a$) is subjected to large bearing and compressive stresses. Meanwhile, the general zone ($D \times H$) is experienced a dispersion of compressive stresses and lateral tensile stresses. The stresses are evenly distributed for both compressive and tensile stresses at the end of the anchorage.

The PZT-embedded interfaces can be employed to monitor the changes in impedance signals caused by the initial damage in the anchorage under PS. As shown in Fig. 1a, two PZTs are positioned at P1 (close to bearing plate) and at P2 (far from bearing plate) in the anchorage for impedance measurement under PS variations. Figure 1b presents the impedance responses obtained from PZTs at P1 and P2. Generally, the impedance signals of PZT at P1 would be more change than that at P2 since the local position P1 is under higher stress variation, thus enabling the feasibility of the impedance-based method for damage monitoring in the anchorage zone.

Variations in impedance responses under structural damage can be quantified by the root mean square deviation (RMSD), which can be found in Giurgiutiu (1998):

$$RMSD\left(Z, Z^*\right) = \sqrt{\sum_{i=1}^{n}\left[Z^*(\omega_i) - Z(\omega_i)\right]^2 / \sum_{i=1}^{n}\left[Z(\omega_i)\right]^2} \quad (2)$$

where $Z(\omega_i)$ and $Z*(\omega_i)$ are the real-parts impedance signatures measured before and after the damage of the i^{th} frequency, respectively.

3. SMART IMPEDANCE MONITORING IN PSC ANCHORAGE

3.1. Prototype of Smart Rebar and Smart Aggregate

As shown in Fig. 2a-b, two prototypes of PZT-embedded interfaces were proposed to measure changes in impedance signals induced by pristine defects in the anchorage zone. Two configurations of PZTs were selected: PZT-embedded aggregate (smart aggregate) can be viewed in Wang (2016) and PZT-embedded rebar (smart rebar) can be found in Karayannis (2016). For smart rebar (see Fig. 2a), a PZT patch (PZT 5A, a size of $10 \times 6 \times 1$ mm) was soldered with electric wires and mounted on a machined surface of the steel rebar. Then an epoxy layer was applied to cover the PZT on the machined area of rebar (about $12 \times 6 \times 1.5$ mm) to waterproof. For smart aggregate (see Fig. 2b), a PZT 5A patch ($10 \times 10 \times 1$ mm) was welded with electric wires and coated by a 0.5 mm epoxy layer. Then the coated PZT was located at the center of a concrete block (ϕ 26 $\times$ h = 26 mm). A concrete mix without coarse aggregate D_{max} 25 listed in Table 1 was used for the smart aggregate fabrication.

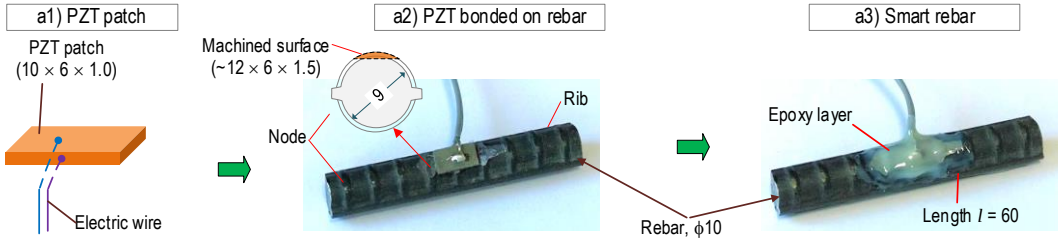

a) PZT-embedded rebar (smart rebar)

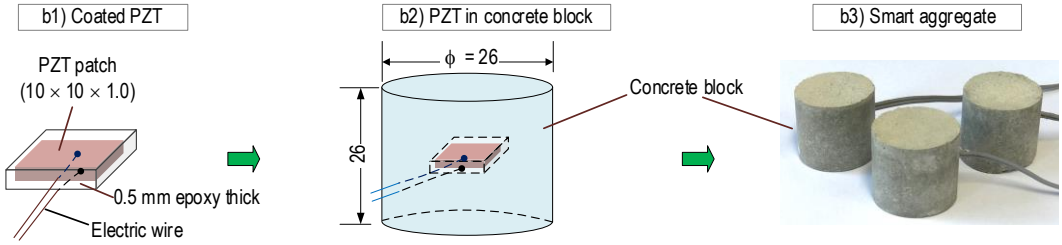

b) PZT-embedded aggregate (smart aggregate)

Fig. 2 Prototype of smart rebar-aggregate for impedance sensing (dimension in mm)

Table 1. Concrete mix for concrete member (*)

Material (1m^3 concrete)	Mass (kg)
Sand	800
Aggregate (Dmax 25)	997
Cement	346
Water	165

(*) The mixture was used for the concrete anchorage zone in Section 3.2

As shown in Fig. 3, impedance signals were measured for a coated PZT, PZT-rebar, and PZT-aggregate. The 1st frequency peak of coated-PZT's impedance was about 190 kHz. It was shifted to about 200 kHz after being formed in the smart aggregate. The magnitude was decreased, which can be referenced in Pham (2021). After formed in the smart rebar, the resonant frequency was shifted to about 280 kHz. The magnitude of impedance signal was reduced, which can be found in Talakokula (2018).

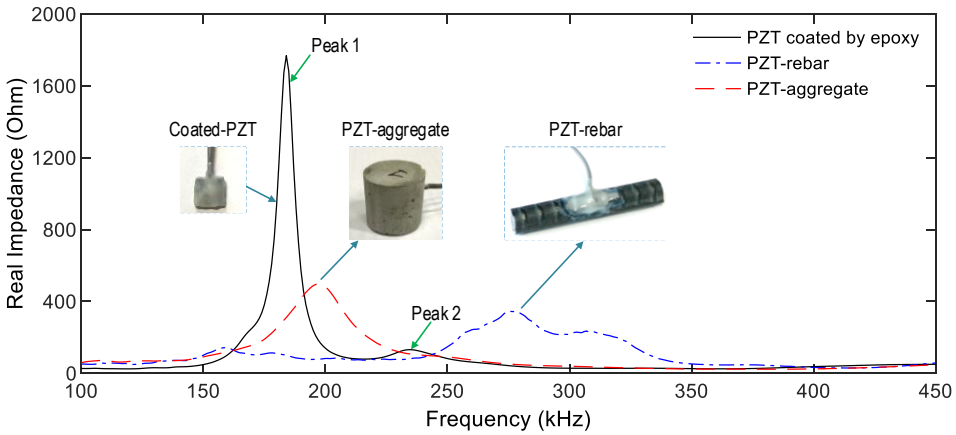

Fig. 3 Measured impedance responses of coated-PZT, PZT-rebar, and PZT-aggregate

3.2. Implementation for Real-Scale PSC Anchorage under Prestress Force

As shown in Fig. 4, a full-scale test on a 9-strands concrete anchorage zone was performed to evaluate the impedance monitoring using smart rebar-aggregate. The anchorage zone consists of an anchor head (ϕ 159 $\times$ h = 75 mm), a bearing plate (200 $\times$ 200 $\times$ 30 mm), and a concrete block (460 $\times$ 460 $\times$ 500 mm) (VSL. International Ltd. (2015)). The detail of the anchorage zone's reinforcement was shown in Fig. 4a: (1) spiral, (2) inner orthogonal stirrups, (3) outer orthogonal stirrups, and (4) longitudinal rebars.

Figure 4a also shows the deployment of smart rebars-aggregates in the anchorage zone during the construction process. Two smart rebars (RB.1-1 and RB.2-1) were installed in two layers of inner stirrups (Rebar 1 and Rebar 2). Rebar 1 and Rebar 2 were placed about 60 mm and 120 mm from the anchorage surface, respectively. Two smart aggregates (AG.1-1 and AG.2-1) were attached to Rebar 1 and Rebar 2, respectively. The anchorage zone was set up on a steel frame to resist tensions induced by prestressing strands (see Fig. 4b). The frame had two steel plates connected via four steel-tubes using bolts. On the left plate, strands were clamped to anchor head by wedges. On the right plate, strands were connected to hydraulic jacks via steel threads, and jacks were used to control tension forces in strands. The applied forces were recorded via 9-load cells.

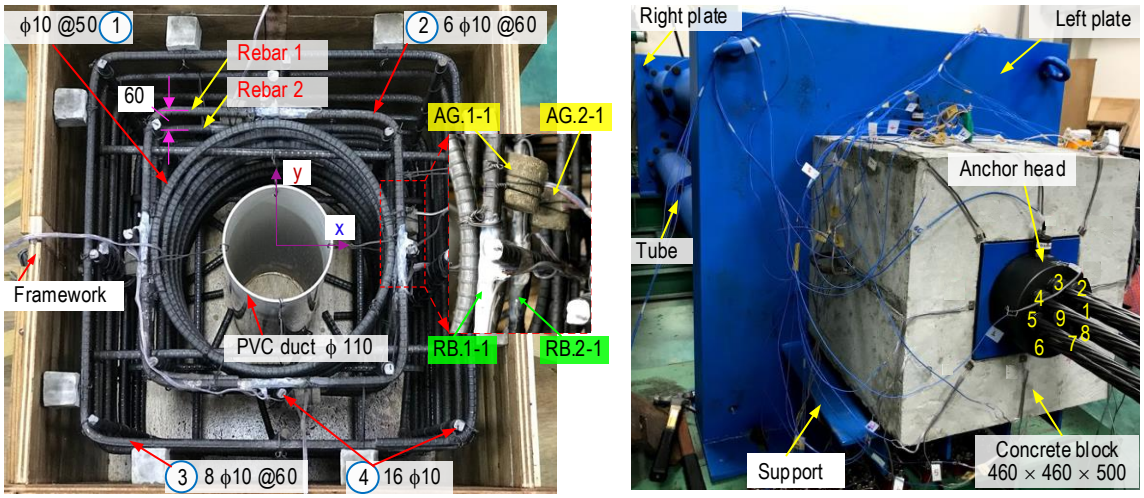

a) Rebar and sensor installation b) Test setup for anchorage zone

Fig. 4 PSC anchorage zone and smart rebar-aggregate (dimension in mm)

Four test cases, namely PS1-PS4, were simulated to measure impedance responses. In PS1, all 9-strands were stressed with a force about 1 kN per strand as the intact baseline, and all load cells were balanced at 0 kN. Then, each strand was increased up to 40 kN for PS2. In PS3 and PS4, each strand was simulated at about 80 kN and 120 kN levels.

For impedance measurement, a wired impedance analyzer was employed to recorded impedance signals from smart rebar-aggregates in the frequency range of 100-600 kHz (501 points). Four ensembles of impedance were measured for each test case to compute the control threshold CL. During the measurement, the lab temperature was controlled around 21.5^{o}C using air conditioners to minimize temperature effects.

As shown in Fig. 5, the impedance signals of smart rebars RB.1-1 and RB.2-1 were

presented in the selected range of 200-400 kHz. RB.1-1 (close to bearing plate) were relatively more sensitive to PS force variation than RB.2-1.

As shown in Fig. 6, the impedance signatures of smart aggregates AG.1-1 and AG.2-1 were presented in the selected range of 100-300 kHz. AG.1-1 (close to bearing plate) were relatively more sensitive to PS force variation than AG.2-1.

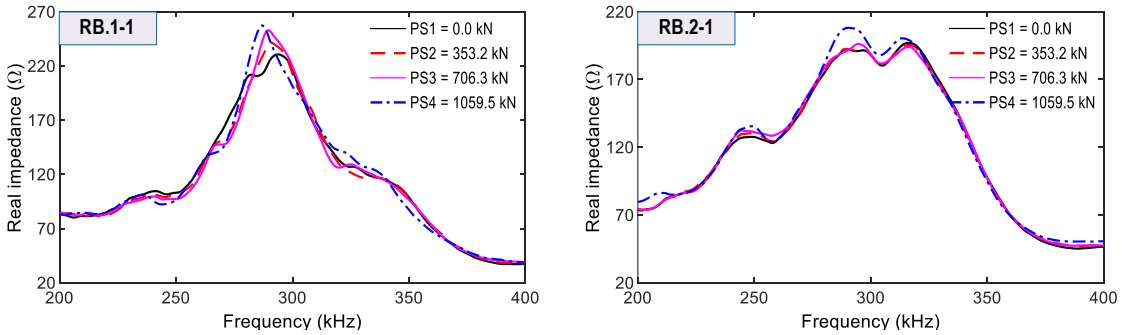

Fig. 5 Impedance responses of smart rebars under prestressing force PS1-PS4

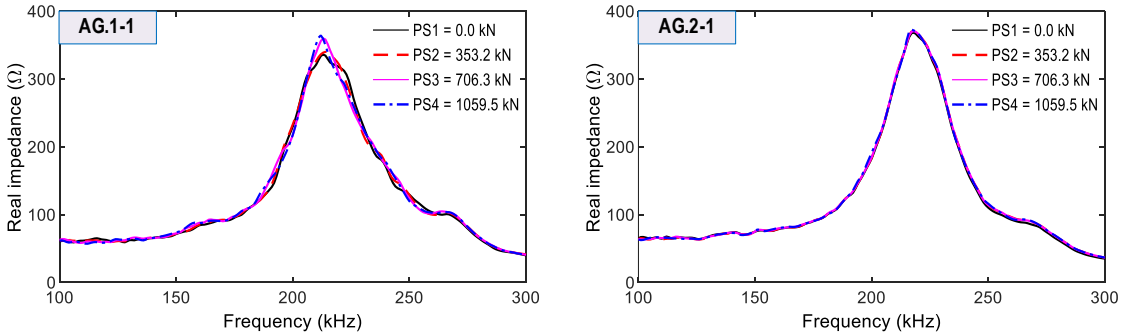

Fig. 6 Impedance responses of smart aggregates under prestressing force PS1-PS4

The change in impedance signatures obtained from smart rebars-aggregates under PS forces was quantified via the RMSD index. Figure 7 shows the RMSD indices of smart rebars under PS1-PS4. In the intact state (PS1), the RMSD magnitudes of smart rebars were relatively small (<1%). The RMSD magnitudes for PS2-PS4 were successively increased and beyond the CL values, thus indicating the variation of PS forces. Furthermore, the RMSD values of RB.1-1 on Rebar 1 were higher than those of RB.2-1 on Rebar 2, confirming that Rebar 1 (placed closer to bearing plate) experienced more stress variation than Rebar 2.

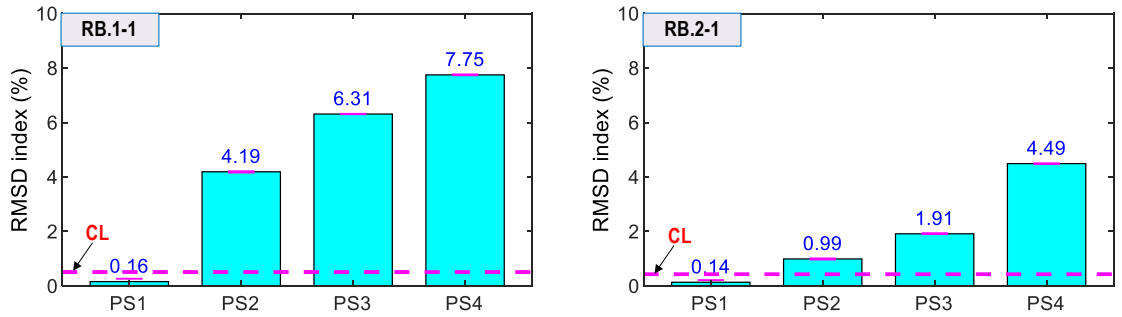

Fig. 7 Impedance features of smart rebars under prestressing force PS1-PS4

Figure 8 shows the RMSD indices of smart aggregates (AG.1-1 and AG.2-1) under PS1-PS4. In the PS1, RMSD indices of smart aggregates were ignorable (<0.6 %). The magnitudes were increased and higher the CL values under loading cases PS2-PS4, thus showing that the smart aggregates successfully detected the variation of prestressing force in the anchorage zone. The RMSD indices of AG.1-1 on Rebar 1 were higher than those of AG.2-1 on Rebar 2.

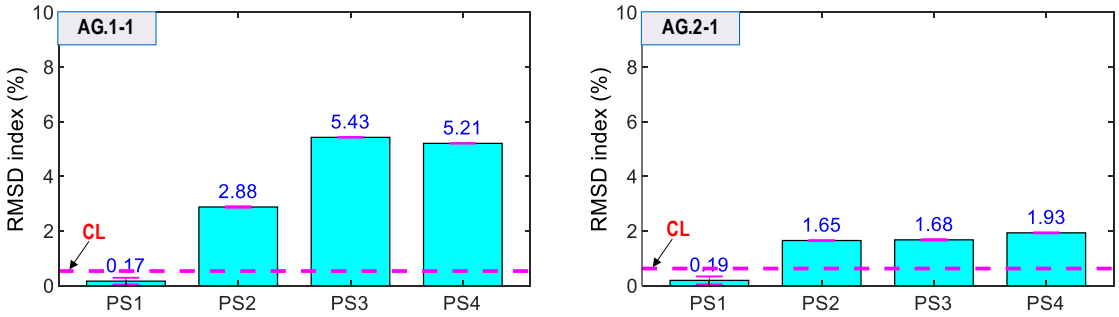

Fig. 8 Impedance features of smart aggregates under prestressing force PS1-PS4

Based on impedance features determined from impedance signals of smart rebars-aggregates, it is suggested that embedded-PZT interfaces should be localized in Rebar 1 to sensitively detect the variation in prestress forces. Furthermore, smart rebars yielded more accurate indications than smart aggregates for the change of applied forces.

4. CONCLUSION

The feasibility of smart rebar-aggregate was investigated for impedance-based monitoring in the PSC anchorage. The impedance-based concept for the anchorage zone via embedded-PZT sensors was illustrated. The prototype of both smart rebar and smart aggregate was designed to obtain impedance signatures. The practicality of the smart rebar-aggregate was evaluated on the real-scale PSC anchorage zone under prestressing force variations.

ACKNOWLEDGMENT

This research was supported by a grant (21CTAP-C163708-01) from the Technology Advancement Research Program funded by Korea Agency for Infrastructure Technology Advancement (KAIA). The post-doctoral researcher and graduate students were also supported by the 4th BK21 program of Korean Government.

REFERENCES

Breen, J.E., Burdet, O., Roberts, C., Sanders, D. and Wollmann, G. (1994). "*Anchorage zone reinforcement for post-tensioned concrete girders*," NCHRP Report 356, Washington, DC: Transportation Research Board.

Marchão, C., Lúcio, V. and Ganz, H.R. (2019). "Efficiency of the confinement reinforcement in anchorage zones of posttensioning tendons," *Struct. Concr.*, **20**(3), 1182-1198.

Bhalla, S. and Soh, C.K. (2004). "Structural Health Monitoring by Piezo–Impedance Transducers. II: Applications," *J. Aerosp. Eng.*, **17**(4), 166-175.

Dang, N.L., Pham, Q.Q. and Kim, J.T. (2020). "Piezoelectric-based hoop-type interface for impedance monitoring of local strand breakage in prestressed multi-strand anchorage," *Struct. Control Health Monit.*, **28**(1), e2649.

Lim, Y.Y., Smith, S.T., Padilla, R.V. and Soh, C.K. (2019). "Monitoring of concrete curing using the electromechanical impedance technique: review and path forward," *Struct. Health Monit.*, **20**(2), 604-636.

Liang, C., Sun, F.P. and Rogers, C.A. (1994). "Coupled Electro-Mechanical Analysis of Adaptive Material Systems-Determination of the Actuator Power Consumption and System Energy Transfer," *J. Intell. Mater. Syst. Struct.*, **5**(1), 335-343.

Ro, K.M., Kim, M.S. and Lee, Y.H. (2020). "Validity of Anchorage Zone Design for Post-Tensioned Concrete Members with High-Strength Strands," *Appl. Sci.*, **10**(9), 3039.

Giurgiutiu, V. and Rogers, C.A. (1998). "Recent Advancements in the Electro-Mechanical (ElM) Impedance Method for Structural Health Monitoring and NDE," *Smart Structures and Materials 1998: Smart Structures and Integrated Systems*, **3329**, 536-547.

Wang, J., Kong, Q., Shi, Z. and Song, G. (2016). "Electromechanical properties of smart aggregate: theoretical modeling and experimental validation," *Smart Mater. Struct.*, **25**(9), 095008.

Karayannis, C.G., Chalioris, C.E., Angeli, G.M., Papadopoulos, N.A., Favvata, M.J. and Providakis, C.P. (2016). "Experimental damage evaluation of reinforced concrete steel bars using piezoelectric sensors," *Constr. Build. Mater.*, **105**, 227-244.

Pham, Q.-Q., Dang, N.-L. and Kim, J.-T. (2021). "Piezoelectric Sensor-Embedded Smart Rock for Damage Monitoring in a Prestressed Anchorage Zone," *Sensors*, **21**(2), 353.

Talakokula, V., Bhalla, S., and Gupta, A. (2018). "Monitoring early hydration of reinforced concrete structures using structural parameters identified by piezo sensors via electromechanical impedance technique," *Mech. Syst. Signal Process.,* **99**, 129-141.

VSL, France (2015). *European technical assessment - VSL Post-Tensioning System.*